Elastic Properties of Amorphous Carbon Networks

Pantelis C. Kelires
Physics Department, University of Crete, P.O. Box 1470, 714 09 Heraklion, Crete, Greece
and Foundation for Research and Technology-Hellas (FORTH), P.O. Box 1527, 711 10, Heraklion, Crete, Greece
(Received 2 June 1994)

We calculated and analyzed for the first time the local atomic stress distributions and the elastic constants of *realistic* amorphous carbon networks. We found that there is always softening of the elastic constants of these isotropic systems, even in the case of nearly tetrahedral coordinations. The local stresses play a very important role in determining the hybridization of a site during the formation of the amorphous phase.

PACS numbers: 61.43.Dq, 62.20.Dc

Amorphous carbon (*a*-C) materials [1], ranging from soft and semimetallic evaporated films (*e*-C) to hard, wide-band-gap, and highly tetrahedral diamondlike films (*ta*-C), attracted much attention in recent years because of practical importance. From a fundamental point of view these materials are also interesting since they are complex and largely varied. The interplay between sp^2 and sp^3 hybrid bonding contributes mostly to this variation and complexity. Therefore, a vast effort has been devoted to understanding how the mixing and number ratio of sp^2 to sp^3 sites controls the mechanical and electronic properties of *a*-C. However, a number of issues remain unclear. A most interesting subject that needs further study is the dependence of the elastic properties, both macroscopic stiffness and local rigidity, on the variation of local bonding, which is correlated to an average atomic coordination z and to a macroscopic density ρ.

Such behavior of elastic properties has been studied in the past for standard models of network glasses, both in the critical regime $z \simeq z_0$ [2] (at $z_0 = 2.4$ a transition from rigid to "floppy" behavior takes place and the elastic constants vanish), as well as in the regime most relevant to glasses [3], where z is significantly larger than z_0. These standard models, however, which are *"bond-depleted"* networks of decreasing z (one removes bonds at random from a diamond-structure network), describe a rather generic behavior of random networks, but not the actual properties of a particular amorphous structure. For example, they ignore the variation of macroscopic density with z, and they are anisotropic (becoming isotropic only close to z_0), contrary to what we expect from an amorphous material.

Here, we study the elastic properties of *realistic* *a*-C models, simulating a wide range of *unhydrogenated* *a*-C materials, from *e*-C to *ta*-C. We estimated, for the first time, the elastic constants (indicative of macroscopic stiffness) of these networks and give their variation with coordination z. We also calculated the local atomic level stresses (pertained to local incompatibilities and rigidity) in these structures. It is consistently found that fourfold-coordinated sites are mostly under compressive stress, while threefold sites are under tensile stress. In sp^3-rich *a*-C, sp^2 sites serve to relieve part of the internal strain energy. We find no evidence for a threshold, with applied pressure, in the $sp^2 \rightarrow sp^3$ transition. These results bear importance in understanding the formation and annealing of *ta*-C structures.

The *a*-C models are computer generated by quenching the liquid under various pressures. This procedure is not directly related to the kinetics of the actual growth process, but still it is primarily based on the concept of applied pressure. Such pressure (compression) is produced, during a deposition process, by the incoming and the penetrating surface ions, resulting in stress generation [4] and densification [5] of *a*-C films. In addition, as we previously showed [6,7], the structure factors $S(k)$ and radial distribution functions $g(r)$ of samples generated in this way agree well with experimental data [8,9].

The simulations are done using a continuous-space Monte Carlo (MC) algorithm in the constant-pressure-temperature (N,P,T) ensemble, which allows equilibration of sample density. We start with cubic cells of 216 atoms with periodic boundary conditions. Molten samples are equilibrated at ~9000 K and then cooled to 300 K under various pressures (0.01–3 Mbar) and at inverse rates of up to ~16 (MC steps)/atom K. After quenching, the pressure is removed, and the sample densities are equilibrated by allowing the shape of the cells to vary (minor modification of the cubic structure) while retaining the periodic boundary conditions. In this way one effectively eliminates any *external stresses* in the models, and so the energy is a true minimum at the relaxed configuration. The process is accompanied by a rather significant sp^3 to sp^2 conversion, especially at high applied pressures, of about 10% and the elimination of some unphysical fivefold defects.

To model the energetics, while making the extensive calculations tractable, we use an empirical interatomic potential [10], which has been extensively tested [6,7] and whose strengths and weaknesses are well known. It has been fitted to the energies of various bulk phases of carbon, and so it describes well the energy difference between graphite and diamond (~0.03 eV/atom). Previous calculations [7,11] showed that the potential (despite the

 0031-9007/94/73(18)/2460(4)$06.00

absence of an explicit π bonding term) describes properly the clustering of sp^2 sites in a-C. They are mostly arranged in pairs and clusters larger than pairs (few sixfold rings), but not in large aromatic clusters (fused sixfold rings). This picture is supported by recent work [12] which argues that the disorder potential in the network overwhelms the ordering energies of sp^2 sites, and so it inhibits clustering.

We begin by considering the question whether or not there is a threshold pressure for the formation of sp^3-*rich* a-C. Figure 1 shows the variation of sp^3 content and of sample density with the applied hydrostatic pressure (we relate to intrinsic stresses below). Our data, resulting from a series of calculations, show a continuous phase ($sp^2 \rightarrow sp^3$) transition in a-C and no indications of a threshold pressure. The increase in sp^3 content and density is more rapid at early stages, then steadily continues at a lower rate, and it reaches limiting values at exceedingly high pressures (over 3.0 Mbar, not shown in the figure, with $z \rightarrow \sim 3.9$ and $\rho/\rho_d \rightarrow \sim 94\%$). The overall behavior obviously looks not linear. Robertson also concluded [5,12], by extrapolating from experimental data [13,14], that there exists a continuous phase transition due to the ability of the random network to accommodate a continuous change in sp^3 content, but he assumed a linear behavior (which by extrapolation leads to a 100% sp^3 network at a certain value of hydrostatic pressure or compressive stress). We believe, however, that the formation of a fully sp^3 bonded a-C network is probably inhibited by the strong tendency of carbon for sp^2 bonding. Additionally, strong disorder (inhomogeneous distribution of stress in the sample) favors a mixed phase of a certain degree since, when locally a region is under tensile stress, an sp^2 site is most likely being formed (see below). In fact, the experimental estimates, reported up to date, give an upper sp^3 content of $\sim 85\%$ (*ta*-C) [13], even lower than our values.

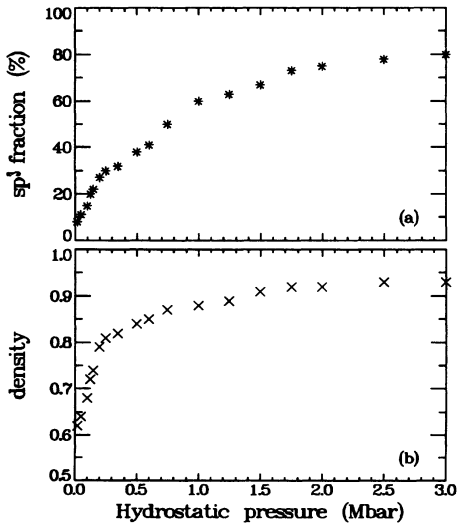

FIG. 1. Variation of (a) sp^3 content and (b) sample density (normalized to diamond's) as a function of applied hydrostatic pressure.

We next proceed to calculate the elastic constants of a-C which have not been estimated before. Calculations are done using standard techniques after cooling the samples to $T = 0$ K at their lowest energy configuration (static-lattice elastic constants). One redefines the supercell with an external strain ϵ, and the elastic modulus c is obtained from the elastic energy $\frac{1}{2}c\epsilon^2$ after all internal degrees of freedom have been fully relaxed. (We still refer to cubic elastic moduli, despite the slight deviation of the cells from cubic symmetry, since this remains valid for a large supercell.) For the calculation of the shear modulus $c_s = c_{11} - c_{12}$, we use a volume conserving orthorhombic strain, while c_{44} is found by shearing the cell with a monoclinic strain (for details see Ref. [15]). The third independent elastic constant, the equilibrium bulk modulus $B_0 = V(d^2E/dV^2)_{V=V_0}$, is obtained by considering a uniform expansion (compression) of the system and fitting points of total energy versus volume with the Murnaghan equation of state for solids.

The results of our calculations are summarized in Table I. Each entry represents the average over three values of each constant, corresponding to the three orientations of each sample. These values should be considered as typically representing pure a-C materials (in the range $3.0 < z < 4.0$). Any fluctuations about them reflect the peculiarities of each amorphous structure, mainly variations of density due to the existence and concentration of voids.

We first note that the structures are mostly isotropic, as is evident from an inspection of the anisotropy parameter $A_{\text{anisotr}} = |c_{44} - (c_{11} - c_{12})/2|$ (values of A_{anisotr} are listed in Table I). The small anisotropy is a result of the finite size of the cells and not due to external stresses (the samples have been fully relaxed). As expected, there is considerable softening of all constants as $z \rightarrow 3.0$ (e-C). The bonding in e-C appears to be locally graphitic (sp^2-like), but with layer warping and interlayer cross-linking, giving a more isotropic character to the network.

TABLE I. Calculated elastic constants (in GPa) and the anisotropy parameter A_{anisotr} for a number of a-C networks distinguished by their coordination z. Also given are the corresponding calculated quantities for the WWW model and for diamond (D).

z	c_{11}	c_{12}	c_{44}	B_0	A_{anisotr}
3.03	446	61	181	189	11
3.20	524	79	218	227	4
3.27	619	81	262	260	7
3.42	691	88	310	289	8
3.50	705	93	312	298	6
3.72	790	101	337	331	7
3.84	834	112	354	353	7
3.89	847	116	357	360	8
WWW	859	118	363	365	7
D	1090	120	640	443	155

(The larger A_{anisotr} for $z = 3.03$ compared to other cells probably indicates some remnants of anisotropic bonding.) This disruption of layers leads to elastic constants which are much softer than the in-plane elastic constants of graphite (known to be very large). With increasing z, c_s (indicative of angular rigidity from hybrid misalignment), and B_0 (indicating radial rigidity) steadily rise and reach high values [16] (~80% of diamond's) for $z \to 3.9$ (*ta*-C). On the other hand, c_{44} attains only ~55% of the diamond value, constrained so by the isotropic character of the network. (The softening of c_{44} in a random lattice can be pictorially understood by viewing the distortion of the sp^3 hybrids under an ϵ_{44} shearing strain [17].)

It is worth examining how much the softening of the elastic constants (from crystalline to amorphous) would be if we had a completely tetrahedral *a*-C network. For this purpose, a hypothetical 100% sp^3 structure is obtained by relaxing the atom positions and cell shape of the 216-atom Wooten-Winer-Weaire (WWW) model [18] with the present carbon potential. The relevant data for this model are listed in Table I. We see that the elastic constants of this isotropic tetrahedral network still remain lower than those of diamond. We thus conclude that the softening, relative to diamond, of highly tetrahedral structures (*ta*-C) primarily originates from the random orientation of the sp^3 hybrids and the accompanying lowering of density, rather than merely from the presence of a small fraction of sp^2 sites.

We now turn to the second elastic property of interest, the *atomic level stresses,* which are a measure of the local rigidity of the network. In a macroscopically rigid network, under no external forces, the local stresses can be thought of as arising due to local incompatibilities, and they are present in networks with nonequivalent atoms and in any disordered structure. One formally defines [19] an atomic level stress tensor associated with an atom at a certain position as the average of the stress field (operating at each point in space) over the atomic volume. It has been proved [20], however, very useful to deal with the trace of this stress tensor, which defines a local compression, and which is quite appropriate for isotropic systems, as is the case here. In this scheme, one considers an atomic compression (tension) $\sigma_i = -dE_i/d\ln V \sim p\Omega_i$, where E_i is the energy of atom i (as obtained by decomposition of the total energy into atomic contributions), and V is the volume. Dividing by the appropriate atomic volume, Ω_i converts into units of pressure. Summing up the σ_i over the atoms of the system we get the total internal stress, which could be zero if the individual contributions cancel each other.

We first apply this methodology to a typical *ta*-C sample with $z = 3.84$ and $\rho/\rho_d = 94\%$. The results of our analysis are portrayed in panel (a) of Fig. 2 which shows the distributions of atomic stresses. (Averages are taken at 300 K, so there is some thermal broadening.) $P(\sigma)$ is the probability of finding an atom under stress σ. The total distribution (denoted by the solid line) is

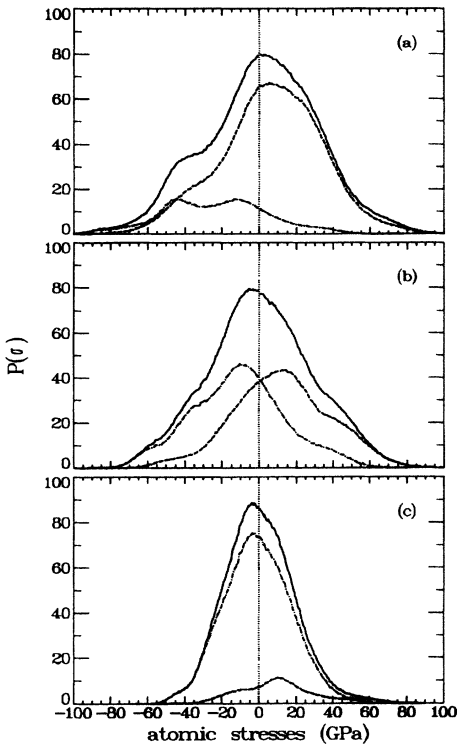

FIG. 2. Distributions $P(\sigma)$ of atomic stresses at 300 K. Solid lines denote total distributions. Dashed and dash-dotted lines are projected distributions for fourfold- and threefold-coordinated atoms, respectively. (a) $P(\sigma)$ for a *ta*-C sample. (b) $P(\sigma)$ for a sample with $z \simeq 3.5$. (c) $P(\sigma)$ for an *e*-C sample.

widespread, indicating the presence of large internal local stresses, compressive as well as tensile. The tails of the distribution originate from atoms having severely strained bonds and angles, and which are weakly bonded (they have high atomic energies [6]). The distribution is peaked at a slightly compressive stress, showing that in this equilibrated sample compressive and tensile stresses nearly balance each other. It is important to note, however, that what is crucial in this analysis is not the average internal stress, but the local stress at each specific site.

We gain more insight into this issue by decomposing the total distribution into contributions from individual atoms according to their coordination [6]. Such a decomposition is shown by the broken lines in Fig. 2(a). As expected, both distributions of fourfold and threefold atoms are quite broad and with fourfold atoms contributing the most to $P(\sigma)$. Interestingly, however, we notice that most of the sp^3 atoms are under compressive stress [as one easily verifies by integrating over the distribution, $N = \int P(\sigma)\,d\sigma$]. The peak value is ~10 GPa. The reported intrinsic compressive stresses in *ta*-C, although macroscopic properties are not directly comparable with the local stresses calculated here, acquire similar values [5,13]. On the other hand, the sp^2 sites are mostly under tensile stresses, whose magnitudes are on the average larger than those of sp^3 sites. This indicates that in this mixed

phase the sp^2 sites, which are assembled in small clusters as noted above, play the role of relieving internal strain energy. Thus, there is a tendency, through densification [5] and compressive stress generation [4], to promote sp^3 bonding, but a certain fraction of sp^2 sites is needed to reduce the total strain in this high energy phase [6].

To eliminate the possibility that these findings are peculiar to the above particular structure, we apply the same analysis to a sample with $z \simeq 3.5$ and $\rho/\rho_d = 87\%$. The results are displayed in Fig. 2(b). Again, we most clearly see the preference of sp^3 sites for compressive and of sp^2 sites for tensile stresses. Therefore, what determines the hybridization at a particular site is not the average total intrinsic stress (which could be zero), but the local atomic stress generated during deposition when the incoming ions stick on the surface (environment favoring neutral or tensile stress, thus sp^2 bonding) or when they penetrate into deeper layers and occupy interstitial positions (compressive conditions favoring sp^3 bonding).

The same pattern is followed even in the case of a low-pressure sample (e-C) having $z \simeq 3.03$ and $\rho/\rho_d = 65\%$. The majority sp^2 sites have a maximum probability to be under a slightly tensile stress ($\simeq$3 GPa), while fourfold sites are mostly compressed and evidently more distorted, in agreement with previous work [6] based on energy considerations. Note also how strain is reduced when moving from ta-C to e-C [panels (a)–(c) in Fig. 2], which is consistent with the lowering of energy as z decreases [6]. Robertson suggested [12] that the free energy difference ΔG between sp^2 and sp^3 a-C can be viewed as being the work done by the incident ions in compressing a low density sp^2 network into a higher density sp^3 network, $W = \Delta G = P\Delta V$. Using for $P \simeq 15$ GPa (the peak value difference of stress among ta-C and e-C in Fig. 2) and the appropriate $\Delta V = 0.69$ among the two samples, we estimate for $\Delta G = 0.17$ eV/atom. This is consistent with the typical total energy differences between ta-C and e-C ($\simeq$0.2 eV/atom) found previously [6].

Finally, we have investigated the issue of thermal annealing of stress in a-C. This is related to the proposed [5] annealing of the density excess (within the thermal spike model), when the incoming ion energies exceed a certain threshold [13,14] (*in as-grown films*). Analyzing a number of samples, we consistently find that, upon annealing, relaxation of density is accompanied by the elimination of many sp^3 sites which are mostly under tensile stress, while compressive stress is harder to anneal out. Fourfold atoms under tension are in a shallow minimum of the free energy (we estimate a difference of ≥ 0.5 eV compared to compressed sp^3 sites). Similar arguments apply to the case of *post-growth* thermal annealing of ta-C structures, which were predicted [6] to be metastable, exhibiting an abrupt $sp^3 \rightarrow sp^2$ transition at $T_{tr} \simeq 1200$ K (seemingly verified by experiment [21]). We expect that at $\sim T_{tr}$ most sp^3 atoms under tension transform into sp^2 sites. Compressed sp^3 atoms are eliminated at higher temperatures.

In conclusion, our numerical analysis gives insights into the issues of elastic softening and local stress distributions in interesting forms of a-C. We believe that further studies are needed to illuminate the relation between strain relaxation and clustering of sp^2 sites in a mixed phase, as well as to understand better the $sp^3 \rightarrow sp^2$ transition above T_{tr}.

[1] For an overview of a-C properties, see J. Robertson, Surf. Coatings Technol. **50**, 185 (1992); Diamond Relat. Mater. **1**, 297 (1992).

[2] H. He and M. F. Thorpe, Phys. Rev. Lett. **54**, 2107 (1985).

[3] D. S. Franzblau and J. Tersoff, Phys. Rev. Lett. **68**, 2172 (1992).

[4] D. R. McKenzie, J. Vac. Sci. Technol. B **11**, 1928 (1993).

[5] J. Robertson, Diamond Relat. Mater. **3**, 361 (1994).

[6] P. C. Kelires, Phys. Rev. Lett. **68**, 1854 (1992); Phys. Rev. B **47**, 1829 (1993).

[7] P. C. Kelires, C. H. Lee, and W. R. Lambrecht, J. Non-Cryst. Solids **164–166**, 1131 (1993).

[8] F. Li and J. Lannin, Phys. Rev. Lett. **65**, 1905 (1990).

[9] K. W. R. Gilkes, P. H. Gaskell, and J. Yuan, J. Non-Cryst. Solids **164–166**, 1107 (1993).

[10] J. Tersoff, Phys. Rev. Lett. **61**, 2879 (1988).

[11] C. H. Lee, W. R. Lambrecht, B. Segall, P. C. Kelires, T. Frauenheim, and U. Stephan, Phys. Rev. B **49**, 11 448 (1994).

[12] J. Robertson, Pure and Appl. Chem. (to be published).

[13] D. R. McKenzie, D. Muller, and B. A. Pailthorpe, Phys. Rev. Lett. **67**, 773 (1991); D. R. McKenzie *et al.*, Diamond Relat. Mater. **1**, 51 (1991).

[14] P. J. Fallon, V. S. Veerasamy, C. A. Davis, J. Robertson, G. Amaratunga, W. I. Milne, and J. Koskinen, Phys. Rev. B **48**, 4777 (1993).

[15] M. J. Mehl, J. E. Osburn, D. A. Papaconstantopoulos, and B. M. Klein, Phys. Rev. B **41**, 10 311 (1990).

[16] The values for B_0 are less than those previously estimated in Ref. [6]. The latter represent an upper limit in the presence of external stresses (no relaxation of cubic boundary conditions).

[17] W. A. Harrison, *Electronic Structure and the Properties of Solids* (W. H. Freeman and Company, San Francisco, 1980), p. 191.

[18] F. Wooten, K. Winer, and D. Weaire, Phys. Rev. Lett. **54**, 1392 (1985).

[19] V. Vitek and T. Egami, Phys. Status Solidi (b) **144**, 145 (1987).

[20] P. C. Kelires and J. Tersoff, Phys. Rev. Lett. **63**, 1164 (1989).

[21] V. S. Veerasamy, G. A. J. Amaratunga, W. I. Milne, J. Robertson, and P. J. Fallon, J. Non-Cryst. Solids **164–166**, 1111 (1993).